European Journal of Neuroscience, Vol. 12, pp. 4573–4577, 2000

SHORT COMMUNICATION
Identification of the target neuronal elements in electrical deep brain stimulation

Jan Holsheimer[1], Hilde Demeulemeester,[2] Bart Nuttin[2] and Paul de Sutter[2]
[1]Institute for Biomedical Technology, University of Twente, PO Box 217, NL-7500 AE Enschede, The Netherlands
[2]Department of Neurological Surgery, University Hospital Gasthuisberg, Leuven, Belgium

Keywords: pallidum stimulation, Parkinson patients, strength–duration time constant, thalamus stimulation, tremor

Abstract

The aim of this study is to identify the primary neuronal target elements in electrical deep-brain stimulation, taking advantage of the difference in strength–duration time constant (τ_{sd}) of large myelinated axons (≈ 30–200 μs), small axons (≈ 200–700 μs) and cell bodies and dendrites (≈ 1–10 ms). Strength–duration data were measured in patients suffering from Parkinson's disease or essential tremor and treated by high-frequency stimulation in the ventral intermediate thalamic nucleus or the internal pallidum. Threshold voltages for the elimination of tremor were determined at various pulsewidths and a pulse rate of 130 pulses per second. The τ_{sd} was calculated using Weiss's linear approximation. Its mean value was 64.6 ± 25.4 μs (SD) for the thalamic nucleus and 75.3 ± 25.5 μs for the internal pallidum. Corrections to the mean values were made because the τ_{sd} values were based on voltage–duration measurements using polarizable electrodes. Apart from this systematic error, a resolution error, due to the relatively large increment steps of the pulse amplitude, was taken into account, resulting in mean τ_{sd} estimates of 129 and 151 μs for the thalamic nucleus and the internal pallidum, respectively. It is concluded that the primary targets of stimulation in both nuclei are most probably large myelinated axons.

Introduction

Electrical deep-brain stimulation (DBS) is a relatively new therapeutic method applied in, for example, the management of persistent pain (Gybels & Sweet, 1989) and the alleviation of essential tremor, Parkinson tremor and other symptoms related to Parkinson's disease (Benabid *et al*., 1993; Gross *et al*., 1997; Benabid *et al*., 1998). Recently Nuttin *et al*. (1999) have shown that symptoms related to obsessive–compulsive neurosis can be relieved by DBS as well. These applications of DBS most probably have in common that the applied electrical stimuli modulate the signal transmission in parts of the neuronal circuitry involved, thereby affecting the related symptoms. This results in, e.g., the alleviation of pain by a synaptically mediated inhibition of ascending nociceptive signal transmission (Yaksh, 1988; Gybels & Sweet, 1989) or the elimination of tremor by inhibiting the signal transmission in the subthalamic nucleus or the internal pallidum (Benazzouz *et al*., 1995; Boraud *et al*., 1996). To advance improvements of these neuromodulatory intervention techniques the underlying neurophysiological mechanisms should be well understood. A primary aspect is the identification of the neuronal elements being targeted by DBS. Target elements could be cell bodies, dendrites or large- or small-diameter axons.

A biophysical parameter allowing a distinction between these target elements is the strength–duration time constant (τ_{sd}), or chronaxie. τ_{sd} has substantially different values for axons and other parts of a neuron. Ranck (1975) concluded that τ_{sd} of cell bodies and dendrites of most neurons is in the 1–10 ms range, i.e. ≈ 50× larger than τ_{sd} of (large) myelinated fibres (30–200 μs). Nowak & Bullier (1998a) obtained similar ratios between τ_{sd} values determined for direct cell body stimulation (mean = 15 ms) and stimulation in both white matter (271 μs) and grey matter (380 μs) of the rat visual cortex. They concluded that a postsynaptic response obtained upon electrical stimulation in the cortical grey matter results from the activation of (small) axons rather than from cell bodies.

Generally, constant-current pulses are applied in strength–duration measurements, because these pulses induce a constant electric field in the target tissue, even when polarizable electrodes are used. Constant-voltage pulses are applied as well (Ranck, 1975), but such pulses will only result in a correct estimate of τ_{sd} if the electrode impedance is invariable, i.e. when nonpolarizable electrodes are used. Unfortunately, constant-current stimulators and nonpolarizable electrodes are not always available, particularly in implantable stimulation systems for clinical use.

In this clinical study strength–duration measurements were made in patients treated by high frequency DBS primarily for essential tremor and Parkinson tremor. The implanted stimulation systems delivered constant-voltage pulses and had polarizable electrodes. Because the corresponding τ_{sd} values were 30–40% lower than when obtained with constant-current pulses (Holsheimer *et al*. 2000), the τ_{sd} values were adjusted accordingly. Preliminary results have been presented by Demeulemeester *et al*. (1998) and Holsheimer *et al*. (1998).

Correspondence: Dr Jan Holsheimer, as above.
E-mail: j.holsheimer@el.utwente.nl

Received 26 January 2000, revised 7 September 2000, accepted 15 September 2000

Materials and methods

Voltage–duration measurements

Voltage–duration (*V–t*) data were measured in patients suffering from Parkinson's disease or essential tremor. For the elimination of tremor most patients had a DBS lead (model 3387, Medtronic, Inc., Minneapolis, MN, USA) placed stereotactically in the ventral intermediate thalamic nucleus (VIM) on one side or bilaterally (Benabid *et al.*, 1993). In some other patients a single DBS lead had been placed in the internal globus pallidus (GPi) for the elimination of rest tremor, rigidity, akinesia and/or for the treatment of dyskinesia (Gross *et al.*, 1997).

The DBS lead had four 1.5-mm-long cylindrical electrodes separated by 1.5 mm on the surface of a polyurethane tube of 1.27 mm diameter. The lead was connected to a subcutaneous, battery powered, voltage-driven pulse generator (Itrel2® or Itrel3®, Medtronic). Pulses were biphasic and charge-balanced. The second phase started 0.3 ms after the end of the first one and had an amplitude of only a few percent of the first phase and a duration of several ms. Pulse width (*PW*), pulse rate, voltage and electrode connections were set by an external programmer (model 7432, Medtronic). The load impedance was measured at a pulse amplitude of 1.0 V and $PW = 0.21$ ms.

All patients provided witnessed informed consent. The study protocol was approved by the Review Board of the Gasthuisberg Hospital. At the time the *V–t* measurements were made, the patients had been on a stable dose of medication for at least one month. Pulses were applied between two electrodes (bipolarly) at a rate of 130 p.p.s. (pulses per second). During a test session threshold voltages (V_{th}) for the elimination of tremor were determined in each patient at $PW = 60$, 90, 120, 150, 180, 210, 300 and 450 μs by increasing the pulse amplitude in 0.1-V steps until the tremor vanished completely, which occurred within 2–3 s after stimulus onset. *PW*s were applied in a random order. Each next stimulation (with a different *PW*) was only started when the tremor had fully recovered.

The way the presence of tremor was determined remained constant throughout a test session for each patient. Among patients, however, the test procedure could differ depending on the type of tremor. When, during a test session, a change in symptomatology was observed between stimulation off periods, the complete set of *V–t* data was excluded from this study.

Calculation of the strength–duration time constant

Weiss (1901) presented the following empirical relationship ('Weiss's law') between *PW* and the threshold charge (Q_{th}) of a stimulus pulse required for the excitation of a nerve fibre

$$Q_{th} = I_{rh} (PW + \tau_{sd}) \quad (1)$$

in which I_{rh} is the rheobase current, defined as the minimum stimulus current needed with a large *PW*. Strength–duration curves are characterized by a reduction of the threshold current (I_{th}) when *PW* is increased. When substituting Q_{th} in equation 1 by $I_{th} \times PW$, the nonlinear current–duration relationship is given by

$$I_{th} = I_{rh} (1 + \tau_{sd}/PW) \quad (2)$$

Because the linear equation 1 has been shown to correlate very well with strength–duration data of both peripheral (Mogyoros *et al.*, 1999) and (Nowak & Bullier, 1998a) central nerve fibres, reliable estimates of I_{rh} and τ_{sd} are provided by the slope of the linear regression line and the intercept of this line with the *PW*-axis, respectively.

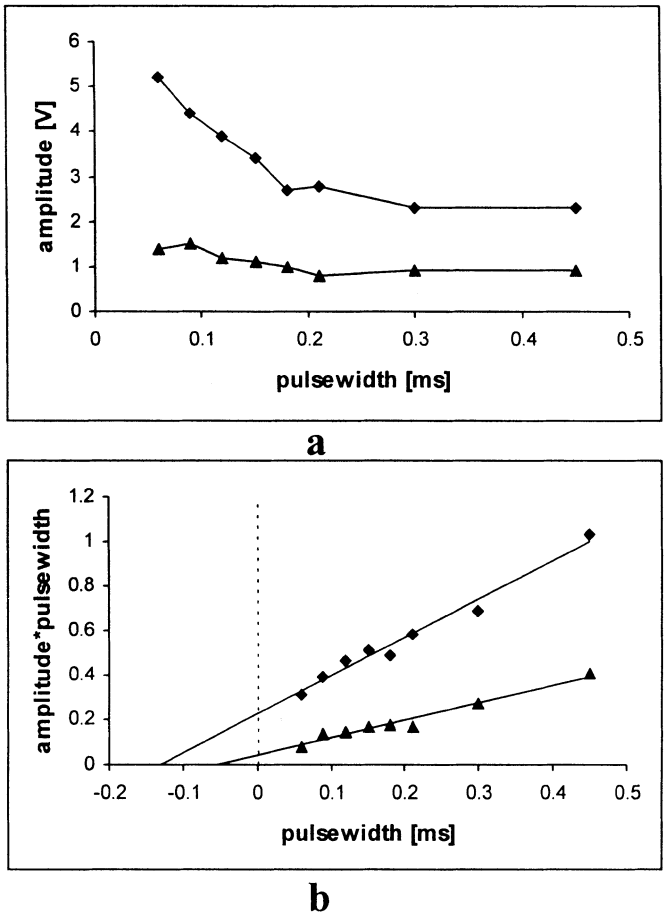

FIG. 1. Voltage–duration data from two subjects (■ and ▲) stimulated in VIM. (a) Plots of pulse amplitude vs. duration; (b) plots of the product of amplitude and duration vs. duration; the strength–duration time constant and the rheobase voltage of each data set correspond to the intercept of the linear fit with the horizontal axis and the slope of this line fit, respectively.

Equation 1 was modified to calculate τ_{sd} and the rheobase voltage (V_{rh}) from the measured *V–t* data. When assuming that the load of the constant-voltage pulse generator is constant, V_{th} is proportional to I_{th} and equation 1 can be written as

$$V_{th} PW = V_{rh} PW + V_{rh} \tau_{sd} \quad (3)$$

The $V_{th} \times PW$ was computed and graphs were made as a function of *PW*. A linear regression line fitting the data points best (minimum root mean square error) was calculated, as well as the corresponding squared correlation coefficient (R^2), and finally V_{rh} and τ_{sd} were determined according to equation 3.

Results

The *V–t* and load impedance measurements were performed on 19 patients. Due to a change in symptomatology during the test session, the data of four patients were excluded from further analysis. Of the remaining patients eight had a single DBS lead and three had bilateral leads in VIM, whereas four patients had a single lead in GPi. Some *V–t* measurements were repeated after a few months, either because the previous test did not provide reliable data, or to test the reproducibility of the measurement. This resulted in a total of 26 *V–t* measurements. The results of *V–t* measurements on two patients are shown in Fig. 1. In Fig. 1a the measured *V–t* data are presented,

TABLE 1. Numbers of patients with unilateral and bilateral DBS leads in VIM/GPi, and numbers of repeated measurements

	VIM unilateral	VIM bilateral	GPi unilateral
Patients	9	2	3
Repeated measurements	1	1	2

whereas in Fig. 1b the data transformed according to equation 3 are shown.

The selection of reliable data was based on R^2 of the measurement data and the linear fit according to equation 3. Twenty-two *V–t* measurements had R^2 values of 0.85–0.99 (mean 0.95). Four measurements had R^2 values < 0.7 (0.30–0.64) and were excluded from further analysis. The τ_{sd} values calculated from the remaining *V–t* measurements varied from 32.7 to 128.9 μs (mean = 67.2 μs), except for a very low value (13.6 μs) and a negative one (–2.7 μs). The latter were also excluded, thus resulting in 20 *V–t* measurements on 14 patients (including four repeated measurements), as shown in Table 1. These data included two measurements on a patient with a DBS lead in GPi, in whom a gait problem instead of tremor was the symptom eliminated by the stimulation. The corresponding parameters τ_{sd}, V_{rh} and R^2 were within the range calculated for the tremor-related *V–t* data.

The results are summarized in Table 2 for data from VIM and GPi separately. It is shown that neither τ_{sd} nor V_{rh} are significantly different for VIM and GPi. The linear fit of the VIM *V–t* data was better than that of GPi. The τ_{sd} and V_{rh} values of the four repeated measurements were different from the initial values. The lower value of τ_{sd} in each patient was 19–41% less than the higher one, whereas the lower value of V_{rh} was 17–65% less. Similar differences were obtained for τ_{sd} and V_{rh} in the two patients with bilateral leads in VIM. Load impedance measurements were only made in 50% of the patients and no significant differences between VIM and GPi were shown.

We also analysed whether the parameters τ_{sd}, V_{rh} and load impedance were related. However, no correlation was observed between τ_{sd} and V_{rh} ($R^2 = 0.07$, $n = 15$ VIM), τ_{sd} and load ($R^2 = 0.17$, 10 VIM + GPi data), and V_{rh} and load data ($R^2 = 0.00$, $n = 10$ VIM + GPi).

In most *V–t* measurements the voltages were rather low. Particularly at larger *PW*s, pulses were almost always < 2 V. Because the increment steps of the pulse amplitude were 0.10 V, the resolution error of V_{th} was rather large and would often result in an overestimation of V_{th}. If, e.g., the measured V_{th} were 0.70 V, the real V_{th} could be 0.61 V or any value in between. Considering that the error in the *y*-values in Fig. 1b is proportional to *PW* and to the error in V_{th}, an overestimation of V_{th} would change the slope of the line most, and thus τ_{sd} and V_{rh}, when related to a large *PW*. The effect of a 0.09-V reduction of V_{th} (at PW = 0.45 V) on τ_{sd} was calculated for several data sets having different V_{rh} values (0.71–2.07 V). In all cases the effect was an increase of τ_{sd}, being 30–50% for small V_{rh} values and ≈ 20% for large values. A 0.09-V reduction of V_{rh} corresponding to $PW = 0.30$ ms resulted in an increase of τ_{sd} by $< 10\%$.

TABLE 2. Means, SDs and minimum/maximum values of τ_{sd}, V_{rh} and R^2 of the *V–t* measurements in VIM and GPi and the load impedance

	τ_{sd} (μs)		V_{rh} (v)		R^2		Load (Ω)	
	VIM	GPi	VIM	GPi	VIM	GPi	VIM	GPi
Mean	64.6	75.3	1.35	1.69	0.97	0.88	1297	1325
SD	25.4	25.5	0.57	0.36	0.02	0.03	185	253
Minimum	32.7	37.3	0.71	1.27	0.92	0.85	1068	1034
Maximum	128.9	104.9	2.55	2.15	0.99	0.94	1540	1491
n	15	5	15	5	15	5	7	3

Discussion and conclusions

Strength–duration time constants

The *V–t* measurements were performed on patients being treated with DBS for motor disorders to determine the corresponding τ_{sd} values, which are indicative of the type of neuronal target element (large or small axons, cell bodies, dendrites). The mean values (± SD) for VIM and GPi stimulation were 64.6 ± 25.4 and 75.3 ± 25.5 μs, respectively, indicating that the τ_{sd} values obtained from the two areas did not differ significantly.

Due to the nonlinear relationship between stimulation voltage and current, caused by the complex impedance of the polarizable DBS electrode (varying with both *PW* and voltage), the *V–t* measurements led to biased τ_{sd} values. In a previous study we demonstrated that τ_{sd} values obtained from *V–t* measurements using a DBS lead are 30–40% below the correct values, i.e. obtained from constant-current measurements (Holsheimer *et al*. 2000). Taking into account an average reduction of τ_{sd} by 35% when calculated from *V–t* data, the correct mean values would have been 99.4 and 116 μs for VIM and GPi, respectively.

A second error arose from the limited resolution of the stimulation voltage (0.1 V). We calculated that a correction for the maximum measurement error (a 0.09-V overestimation at $PW = 0.45$ ms) results in an increase of τ_{sd} by 20–50% (Holsheimer *et al*. 2000). Assuming an average correction of 30%, the corrected mean values of τ_{sd} are 129 and 151 μs for VIM and GPi, respectively.

From these corrected results it is most likely that the primary targets of DBS in VIM and GPi are large myelinated axons, because these axons are known to have a τ_{sd} not exceeding ≈ 0.2 ms, whereas smaller axons have values of ≈ 0.2–0.7 ms and cell bodies, dendrites and small unmyelinated axons have a τ_{sd} exceeding 1 ms (Ranck, 1975; West & Wolstencroft, 1983; Nowak & Bullier, 1998a).

The τ_{sd} values of large axons are 3–4× higher when peripheral nerves are stimulated with surface electrodes (Mogyoros *et al*., 1996), presumably due to the large electrode size (10 mm diameter), the rather large distance from the target fibres and the electrical impedance of the skin. Therefore, we did not compare our data with these values.

Whereas, single pulses are generally applied in the measurement of strength–duration curves, continuous stimulation at a rate of 130 p.p.s. was used in this study. This makes, however, no difference for the conclusions, because the individual pulses are biphasic and charge-balanced.

Factors affecting the strength–duration time constant

The values of τ_{sd} varied considerably, both among subjects (by a factor of 3–4) and among repeated tests in the same subject (up to a factor of 2). A large intersubject and intrasubject variability has also been reported by Mogyoros *et al*. (2000) for cutaneous afferents in the human median nerve.

The variability of τ_{sd} we observed may have several origins. Apart from the variable systematic and resolution errors discussed under 'Strength–duration time constants' section (above), other

factors may affect the variability of τ_{sd} as well. First, a larger distance between electrode and target fibres results in a larger τ_{sd} (West & Wolstencroft, 1983). This relationship was also observed in computer modelling of spinal cord stimulation (J. J. Struijk, W. A. Wesselink & J. Holsheimer, unpublished data). Because among patients DBS leads are likely to be situated slightly differently with respect to the target area, their distance to the target fibres may be different as well and may thus contribute to the variability of τ_{sd}. Secondly, an inverse relationship has been demonstrated between τ_{sd} and the conduction velocity of nerve fibers and thus their diameter (West & Wolstencroft, 1983; Swadlow, 1992; Nowak & Bullier, 1998a; Wesselink *et al*., 1999). A variation in size of the target fibres among patients may thus add to the variation of τ_{sd}. Finally, different rates of spontaneous activity in the target fibres may induce different average nodal membrane potentials and τ_{sd} values (Kiernan *et al*., 1997; Vagg *et al*., 1998).

Because both τ_{sd} and V_{rh} rise with increasing distance between the electrode and the target axons, a correlation between the two parameters would be expected. However, no correlation could be demonstrated, which is most probably due to factors affecting τ_{sd} as discussed. Similarly, the expected correlation between load impedance and V_{rh} is most probably disturbed by both a variable size of the target axons and a variable distance between the DBS lead and the target axons.

Neurophysiological mechanism

Because myelinated nerve fibres are most probably the elements in VIM and GPi targeted by DBS, the effect of stimulation may be mediated by both afferents and efferents of these nuclei. According to Nowak & Bullier (1998b) it is likely that responses will primarily result from stimulation of afferent axonal branches, because their density is high compared to the density of efferents and they are most probably innervating many more neurons.

Due to the dominating GABA-mediated input of GPi (striatal and external pallidal efferents) it is likely that the stimulation of afferents in GPi results in an increased inhibitory input of GPi neurons. This mechanism has previously been proposed by Boraud *et al*. (1996). Stimulation at a reduced rate would result in insufficient hyperpolarization to compensate for the spontaneous facilitatory input to the GPi neurons. A similar mechanism is likely to occur in high frequency stimulation of the subthalamic nucleus receiving its major (GABA-mediated) input from the pallidum. An alternative mechanism involving axonal 'depolarization block', as postulated by Benazzouz *et al*. (1995), is unlikely because the stimulation rate (130 p.p.s.) is far below the maximum firing rate of cells in the subthalamic nucleus (500/s) (Nakanishi *et al*., 1987). The induction of a somadendritic membrane depolarization (or hyperpolarization) is not likely either, because trains of biphasic, charge-balanced pulses with a short duration as compared to the somadendritic membrane time constant (> 1 ms) are applied in patients during high frequency stimulation.

As a result of DBS, the spontaneous efferent activity of most neurons in the stimulated pool would be reduced, whereas rather few efferents would be stimulated immediately and generate action potentials at a high rate. In this way a massive modulation of the major output structures of the basal ganglia, sufficient to allow the abolition of tremor, could result from high frequency stimulation.

Abbreviations

DBS, deep-brain stimulation; GPi, internal globus pallidus; *PW*, pulse width; Q_{th}, threshold charge; R^2, squared correlation coefficient; τ_{sd}, strength–duration time constant; VIM, ventral intermediate thalamic nucleus; *V–t*, voltage–duration; V_{rh}, rheobase voltage; V_{th}, threshold voltage.

References

Benabid, A.L., Pollak, P., Seigneuret, E., Hoffmann, D., Gay, E. & Perret, J. (1993) Chronic VIM thalamic stimulation in Parkinson's disease, essential tremor and extra-pyramidal dyskinesias. *Acta Neurochir. Suppl. [Wien]*, **58**, 39–44.

Benabid, A.L., Benazzouz, A., Hoffmann, D., Limousin, P., Krack, P. & Pollak, P. (1998) Long-term electrical inhibition of deep brain targets in movement disorders. *Movement Disorders*, **13** (Suppl. 3), 119–125.

Benazzouz, A., Piallat, B., Pollak, P. & Benabid, A.L. (1995) Responses of substantia nigra pars reticulata and globus pallidus complex to high frequency stimulation of the subthalamic nucleus in rats: electrophysiological data. *Neurosci. Lett.*, **189**, 77–80.

Boraud, T., Bezard, E., Bioulac, B. & Gross, C. (1996) High frequency stimulation of the internal Globus Pallidus (GPi) simultaneously improves parkinsonian symptoms and reduces the firing frequency of GPi neurons in the MPTP-treated monkey. *Neurosci. Lett.*, **215**, 17–20.

Demeulemeester, H., Nuttin, B., Wesselink, W.A. & Holsheimer, J. (1998) Which neuronal elements are activated in deep brain stimulation. *Acta. Neurochir. (Wien)*, **140**, 843–844.

Gross, C., Rougier, A., Guehl, D., Boraud, T., Julien, J. & Bioulac, B. (1997) High frequency stimulation of the globus pallidus internalis in Parkinson's disease: a study of seven cases. *J. Neurosurg.*, **87**, 491–498.

Gybels, J.M. & Sweet, W.H. (1989) Deep brain stimulation. In Gildenberg, P.L. (ed.), *Neurosurgical Treatment of Persistent Pain. Physiological and Pathological Mechanisms of Human Pain: Pain and Headache*, Vol. 11. Karger, Basel, Switzerland, pp. 303–317.

Holsheimer, J., Wesselink, W.A., Dijkstra, E.A., Demeulemeester, H. & Nuttin, B. (1998) The effect of DBS on tremor is mediated by the electrical stimulation of myelinated nerve fibers. *Proceedings of the 4th Congress Int. Neuromodulation Soc., Luzerne.* Int. Neuromodulation Society, Luzerne, Switzerland, p. 287.

Holsheimer, J., Dijkstra, E.A., Demeulemeester, H. & Nuttin, B. (2000) Chronaxie calculated from current-duration and voltage-duration data. *J. Neurosci. Meth.*, **97**, 45–50.

Kiernan, M.C., Mogyoros, I., Hales, J.P., Gracies, J.M. & Burke, D. (1997) Excitability changes in human cutaneous afferents induced by prolonged repetitive axonal activity. *J. Physiol. (Lond.)*, **500**, 255–264.

Mogyoros, I., Kiernan, M.C. & Burke, D. (1996) Strength-duration properties of human peripheral nerve. *Brain*, **119**, 439–447.

Mogyoros, I., Lin, C., Dowla, S., Grosskreutz, J. & Burke, D. (1999) Strength-duration properties and their voltage-dependence at different sites along the median nerve. *Clin. Neurophysiol.*, **110**, 1618–1624.

Mogyoros, I., Lin, C., Dowla, S., Grosskreutz, J. & Burke, D. (2000) Reproducibility of indices of axonal excitability in human subjects. *Clin. Neurophysiol.*, **111**, 23–28.

Nakanishi, H., Kita, H. & Kitai, S.T. (1987) Electrical membrane properties of rat subthalamic neurons in an in vitro slice preparation. *Brain Res.*, **437**, 35–44.

Nowak, L.G. & Bullier, J. (1998a) Axons, but not cell bodies, are activated by electrical stimulation in cortical gray matter. I Evidence from chronaxie measurements. *Exp. Brain Res.*, **118**, 477–488.

Nowak, L.G. & Bullier, J. (1998b) Axons, but not cell bodies, are activated by electrical stimulation in cortical gray matter. II Evidence from selective inactivation of cell bodies and axon initial segments. *Exp. Brain Res.*, **118**, 489–500.

Nuttin, B., Cosyns, P., Demeulemeester, H., Gybels, J. & Meyerson, B. (1999) Electrical stimulation in anterior limbs of internal capsules in patients with obsessive-compulsive disorder. *Lancet*, **354**, 1526.

Ranck, J.B. (1975) Which elements are excited in electrical stimulation of the mammalian central nervous system: a review. *Brain Res.*, **98**, 417–440.

Swadlow, H.A. (1992) Monitoring the excitability of neocortical efferent neurons to direct activation by extracellular current pulses. *J. Neurophysiol.*, **68**, 605–619.

Vagg, R., Mogyoros, I., Kiernan, M.C. & Burke, D. (1998) Activity-dependent hyperpolarization of human motor axons produced by natural activity. *J. Physiol. (Lond.)*, **507**, 919–925.

Weiss, G. (1901) Sur la possibilité de rendre comparables entre eux les appareils servant à l'excitation électrique. *Arch. Ital. Biol.*, **35**, 413–446.
Wesselink, W.A., Holsheimer, J. & Boom, H.B.K. (1999) A model of the electrical behaviour of myelinated sensory nerve fibres based on human data. *Med. Biol. Eng. Comput.*, **37**, 228–235.
West, D.C. & Wolstencroft, J.H. (1983) Strength-duration characteristics of myelinated and non-myelinated bulbospinal axons in the cat spinal cord. *J. Physiol. (Lond.)*, **337**, 37–50.
Yaksh, T.L. (1988) CNS mechanisms of pain and analgesia. *Cancer Surveys*, **7**, 5–28.